IOP Publishing Journal of Physics: Condensed Matter
J. Phys.: Condens. Matter **33** (2021) 365402 (7pp) https://doi.org/10.1088/1361-648X/ac0dd5

Dendritic growth of ice crystals: a test of theory with experiments

L V Toropova[1,2,*], E A Titova[3], D V Alexandrov[1,4], P K Galenko[1,2], M Rettenmayr[2], A Kao[5] and G Demange[6]

[1] Laboratory of Multi-Scale Mathematical Modeling, Department of Theoretical and Mathematical Physics, Ural Federal University, Ekaterinburg, 620000, Russia
[2] Otto-Schott-Institut für Materialforschung, Friedrich-Schiller-Universität Jena, 07743 Jena, Germany
[3] Laboratory of Mathematical Modeling of Physical and Chemical Processes in Multiphase Media, Department of Theoretical and Mathematical Physics, Ural Federal University, Ekaterinburg, 620000, Russia
[4] Sirius University of Science and Technology, 1 Olympic Ave., 354340, Sochi, Russia
[5] Centre for Numerical Modelling and Process Analysis, University of Greenwich, Old Royal Naval College, Park Row, London SE10 9LS, United Kingdom
[6] GPM, CNRS-UMR 6634, University of Rouen Normandy, 76801, Saint Étienne Du Rouvray, France

E-mail: l.v.toropova@urfu.ru

Received 19 March 2021, revised 19 May 2021
Accepted for publication 23 June 2021
Published 9 July 2021

Abstract

Motivated by an important application of dendritic crystals in the form of an elliptical paraboloid, which widely spread in nature (ice crystals), we develop here the selection theory of their stable growth mode. This theory enables us to separately define the tip velocity of dendrites and their tip diameter as functions of the melt undercooling. This, in turn, makes it possible to judge the microstructure of the material obtained as a result of the crystallization process. So, in the first instance, the steady-state analytical solution that describes the growth of such dendrites in undercooled one-component liquids is found. Then a system of equations consisting of the selection criterion and the undercooling balance that describes a stable growth mode of elliptical dendrites is formulated and analyzed. Three parametric solutions of this system are deduced in an explicit form. Our calculations based on these solutions demonstrate that the theoretical predictions are in good agreement with experimental data for ice dendrites growing at small undercoolings in pure water.

Keywords: dendritic growth, selection theory, crystal anisotropy

(Some figures may appear in colour only in the online journal)

1. Introduction

It is well-known that the processes of phase transformation from the metastable and nonequilibrium states underlie the preparation of many materials with specific physicochemical properties. As this takes place, the growth features of dendritic structures evolving in undercooled liquids determine the emerging microstructure of materials obtained in solidification processes [1–6]. For a theoretical description of the stable growth mode of dendritic crystals, the theory of microscopic solvability was originally developed for pure (one-component) melts [7–9], which makes it possible to select the relationship between the growth velocity of a dendrite tip, its radius of curvature, and melt undercooling. This theory is based on two nonlinear equations—the selection criterion and the undercooling balance. Using these algebraic equations, it is possible to independently determine the velocity and radius of curvature of the dendritic tip depending on the system undercooling (the driving force of dendritic growth). Then this theory was extended to binary melts [10, 11], dendritic growth under conditions of convective fluid flow [12–17], and also to processes of local nonequilibrium (rapid) crystallization [18–20].

* Author to whom any correspondence should be addressed.

Figure 1. 3D phase-field simulation of non-axisymmetric ice dendrite growth [21, 22]. From left to right: stellar dendrite with secondary branching, stellar dendrite, fern-like dendrite, and 12-arms star. Reproduced from [22]. CC BY 4.0.

Aside from [21, 22] (see figure 1), the vast majority of theoretical and numerical studies using solvability theory are based on the assumption of axisymmetric dendrite tip (for instance [23]). However, experimental data show that dendritic crystals often represent non-axisymmetric structures, i.e. their tip shapes may have different curvature radii in the basal and perpendicular planes (ice crystals represent a good example of such non-axisymmetric dendrites) [24–28]. These experimental observations have yet never been ensured by a theory that allows selecting a stable growth mode for such crystals. The present work is devoted to the selection theory of non-axisymmetric dendritic crystals growing with various crystalline symmetries in the basal and perpendicular planes. Our approach is based on the analysis of two-dimensional crystal growth, taking into account the fact that the dendritic tip in these planes evolves with the same velocity. The developed theory is tested against experimental data that confirm our theoretical conclusions.

2. Analytical theory

Let us consider the stationary growth of dendrite in the form of an elliptical paraboloid from an undercooled one-component melt (see figure 2). For the sake of simplicity, we neglect the melt flow that could be induced by the temperature and pressure gradients. The elliptical paraboloid is defined by two forming parabolas in perpendicular planes with diameters ρ_6 and ρ_2. Here we mean the growth of ice crystals having six-fold symmetry in the basal plane and two-fold symmetry in the perpendicular plane. Keeping this in mind we use subscripts 6 and 2. Noteworthy, the present theory can be generalized to the growth of a three-dimensional dendritic crystal with another crystalline symmetry (for instance, 6 and 3). Next, assuming that the dendritic interface is isothermal, we describe the temperature field in the melt by a single coordinate that specifies the isothermal surfaces and represents an elliptical paraboloid [29].

In this case, the interface equation in dimensionless coordinates x, y, z takes the form

$$\frac{x^2}{\omega - b} + \frac{y^2}{\omega + b} = \omega - 2z, \tag{1}$$

where the length scale is a $2D_{\mathrm{T}}/V$, D_{T} is the thermal diffusivity, V is a constant growth rate, ω is an isothermal level set variable and $b = (\rho_6 - \rho_2)D_{\mathrm{T}}/V$ is a dimensionless parameter of ellipticity.

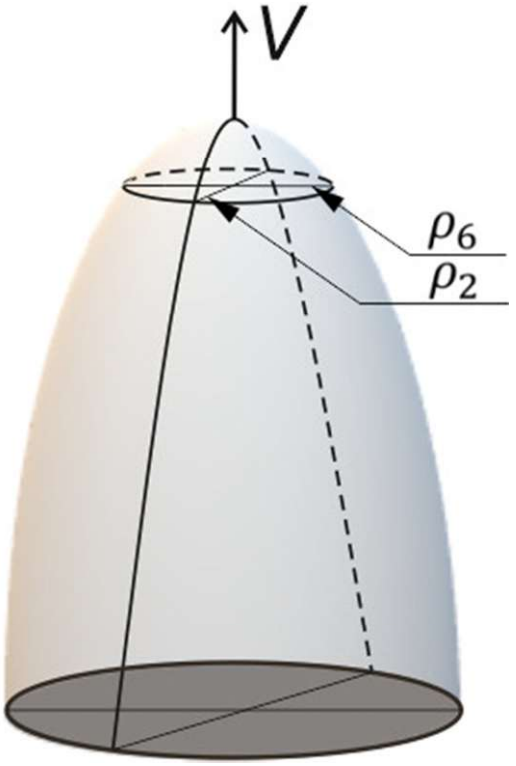

Figure 2. A sketch of tip region of a dendritic crystal in the form of an elliptical paraboloid.

Note that in the case of stationary growth, the dendritic shape is fixed, and the ratio k of its tip diameters is constant, i.e.

$$\frac{\rho + bV/(2D_{\mathrm{T}})}{\rho - bV/(2D_{\mathrm{T}})} = \frac{\rho_6}{\rho_2} = k \geqslant 1. \tag{2}$$

2.1. Selection criterion

The selection criterion allows us to obtain the dendritic growth velocity and tip diameters in two planes of the hexagonal-packed crystal lattice, having the six-fold symmetry in its basal plane and two-fold symmetry in the perpendicular vertical plane. In the 2D and axisymmetric 3D cases, this criterion has been found both analytically and numerically [7, 11]. For the nonaxisymmetric 3D problem, the axisymmetric solution can be used as an approximation in the vicinity of dendritic tip [30]. Thus, to find three parameters, namely the growth velocity V and two dendrite tip diameters ρ_n ($n = 2, 6$), we use two solvability criteria in the two perpendicular planes of the dendrite (basal, where $n = 6$ and vertical, where $n = 2$). Therefore, let us write out the general form of 2D selection criterion for a single-component system without convection as [11–14, 18–20]

$$\sigma^*_n \equiv \frac{2d_0D_{\mathrm{T}}}{\rho_n^2 V} = \frac{\sigma_{0n}\alpha_{dn}^{7/n}A_n^{7/n}}{\left(1 + a_{1n}\alpha_{dn}^{2/n}A_n^{2/n}P_{gn}\right)^2}, \tag{3}$$

where d_0 is the capillary length constant, σ_{0n} is the solvability constant, α_{dn} is the anisotropy parameter (stiffness), n is the order of symmetry (it indicates a concrete crystalline plane),

$P_{gn} = (\rho_n V)/(2D_T)$ is the symmetry-dependent Péclet number and

$$a_{1n} = \sqrt{\frac{8\sigma_{0n}}{7}}\left(\frac{3}{56}\right)^{3/8} A_n^{3/(2n)} \alpha_{dn}^{(12-3n)/(8n)},$$

$$A_n = 2^{-3n/4}\sum_{k=0}^{n}\binom{n}{k} i^{n-k}\cos\frac{(n-k)\pi}{2}$$

(see, for more details, references [13, 26, 31]). It is significant to note that the selection criterion (3) connects the averaged tip diameter $\rho = \rho_6 - b = \rho_2 + b$ and the tip velocity (the rhs also depends on these unknowns through P_{gn}).

2.2. Undercooling balance

The second relation between the growth velocity and tip radii can be retrieved from the undercooling balance representing the driving force of crystal growth. The total undercooling $\Delta T = T_m - T_\infty$ at the dendrite tip consists in several contributions

$$\Delta T = \Delta T_T + \Delta T_R, \tag{4}$$

where T_m is the melting temperature of a planar front, T_∞ is the temperature far from the growing dendrite, and ΔT_T stands for the thermal undercooling, which reads as (see appendix)

$$\Delta T_T = T_Q \exp(P_T)\sqrt{P_T^2 - b^2}\int_{P_T}^{\infty}\frac{\exp(-y)\mathrm{d}y}{\sqrt{y^2-b^2}}. \tag{5}$$

Here $T_Q = Q/c_p$ represents the adiabatic temperature, Q is the latent heat of solidification, c_p is the specific heat, $P_T = (\rho_6 + \rho_2)V/(4D_T)$ is the Péclet number based on the averaged tip diameter $\rho = (\rho_6 + \rho_2)/2$. The curvature contribution ΔT_R stands for the undercooling induced by the Gibbs–Thomson effect, which can be written in the form of

$$\Delta T_R = 2d_0 T_Q\left(\frac{1}{\rho + b} + \frac{1}{\rho - b}\right). \tag{6}$$

Note that the total undercooling balance (4) connects $\rho = \rho_6 - b = \rho_2 + b$, V and ΔT.

Using the stability criterion in two perpendicular planes with a different order of symmetry together with the undercooling balance allows us to have a closed system of three equations with three unknowns (two radii ρ_6 and ρ_2 of forming parabolas and constant growth velocity V).

2.3. Exact analytical solutions

Let us find now the exact analytical solutions of the nonlinear set of three governing equations (3) and (4) in a parametric form. Note that equation (3) represents two selection criteria for the larger (ρ_6) and smaller (ρ_2) dendritic tip diameters ($\rho_6 > \rho_2$). To do this, we first equate the growth rate V expressed in terms of ρ_6 and ρ_2 (see criterion (3)) to each other and obtain $V(\rho_2)$ and $\rho_6(\rho_2)$. Finally, substituting them into the undercooling balance (4), we get the first analytical solution

$$\rho_6(\rho_2) = \frac{1}{\sqrt{V(\rho_2)}\left(\sqrt{\psi_6} - \chi_6\sqrt{V(\rho_2)}\right)},$$

$$V(\rho_2) = \frac{\psi_2\rho_2 - 2\chi_2 - \sqrt{(\psi_2\rho_2 - 2\chi_2)^2 - 4\chi_2^2\rho_2}}{2\chi_2^2\rho_2},$$

$$\Delta T(\rho_2) = T_Q\left[\exp(P_T(\rho_2))\sqrt{\rho_6(\rho_2)\rho_2}\right.$$
$$\times\int_{P_T(\rho_2)}^{\infty}\frac{\exp(-y)\mathrm{d}y}{\sqrt{y^2 - (\rho_6(\rho_2) - \rho_2)^2/4}}$$
$$\left. + 2d_0\left(\frac{1}{\rho_6(\rho_2)} + \frac{1}{\rho_2}\right)\right],$$

$$\chi_n = \frac{a_{1n}\alpha_{dn}^{2/n}A_n^{2/n}}{2D_T},$$

$$\psi_n = \frac{\sigma_{0n}\alpha_{dn}^{7/n}A_n^{7/n}}{2d_0D_T}, \tag{7}$$

where $P_T(\rho_2) = (\rho_6(\rho_2) + \rho_2)V(\rho_2)/(4D_T)$, parameter n equals to 6 or 2, and ρ_2 plays the role of a decision variable (free parameter that can be tunned). Expressions (7) represent the first parametric solution.

The second solution can be found in another parametric space where ρ_6 plays the role of a decision variable. For that purpose, we should replace ρ_2 with ρ_6 and vice versa in expressions (7).

Now choosing V as a decision variable, we come to the third parametric solution of the form

$$\rho_n(V) = \frac{\chi_n\sqrt{V} + \sqrt{\psi_n}}{\sqrt{V}\left(\psi_n - \chi_n^2 V\right)}, \quad n = 2, 6,$$

$$\Delta T(V) = T_Q\left[\exp(P_T(V))\sqrt{\rho_6(V)\rho_2(V)}\right.$$
$$\times\int_{P_T(V)}^{\infty}\frac{\exp(-y)\mathrm{d}y}{\sqrt{y^2 - (\rho_6(V) - \rho_2(V))^2/4}}$$
$$\left. + 2d_0\left(\frac{1}{\rho_6(V)} + \frac{1}{\rho_2(V)}\right)\right], \tag{8}$$

where $P_T(V) = (\rho_6(V) + \rho_2(V))V/(4D_T)$, χ_n and ψ_n are given by expressions (7).

3. Experimental tests

Let us compare the present theory (expressions (8)) with experimental data [24, 25] on the growth of ice crystals (physical parameters are given in table 1). Figures 3–5 illustrate the dendritic tip velocity V and its tip radii in the basal (larger radius ρ_6) and perpendicular to it (smaller radius ρ_2) planes. As is easily seen, the tip velocity monotonously increases and tip radii monotonously decrease when increasing the melt

Table 1. Material and design parameters for dendritic growth.

Parameter	Teraoka *et al* [24]	Yoshizaki *et al* [25]
Capillary constant (d_0, m)	2.8×10^{-10}	2.8×10^{-10}
Thermal diffusivity (D_{T}, $\mathrm{m^2\ s^{-1}}$)	1.34×10^{-7}	1.17×10^{-7}
Melting temperature (T_{m}, K)	273.15	276.90
Hypercooling (T_{Q}, K)	79.67	81.56
Stiffnesses ($\alpha_{d02}/\alpha_{d06}$)	1.5/0.25	1.5/0.20
Solvability constants (σ_{02}/σ_{06})	230/0.0018	245/0.0021

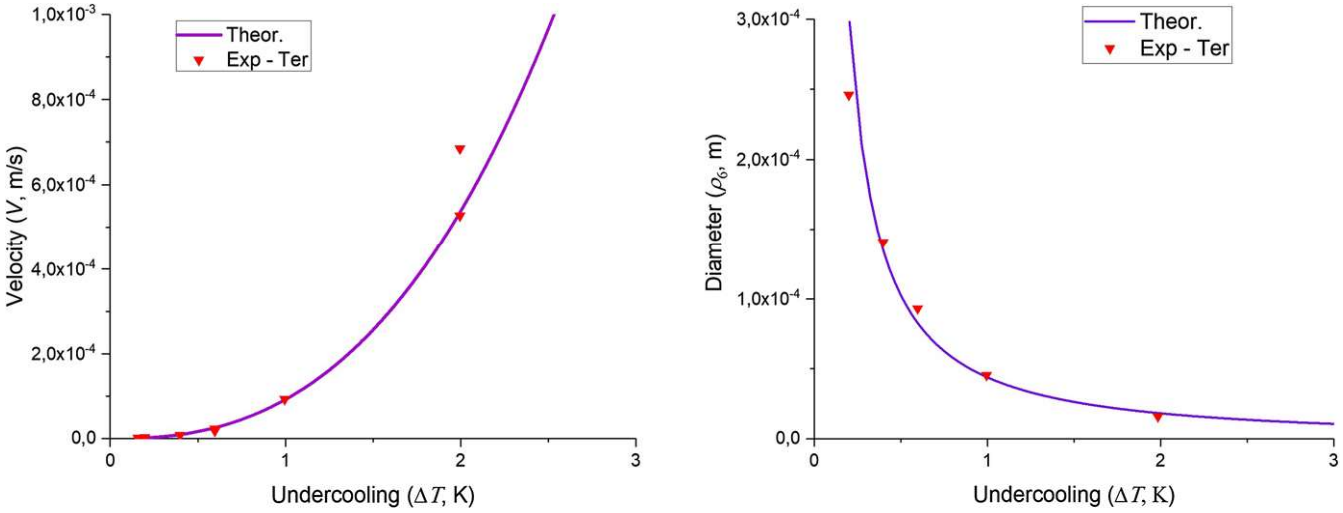

Figure 3. Theory versus experiments carried out by Teraoka *et al* [24] for the dendrite tip velocity V and its larger tip diameter ρ_6 as functions of the melt undercooling ΔT.

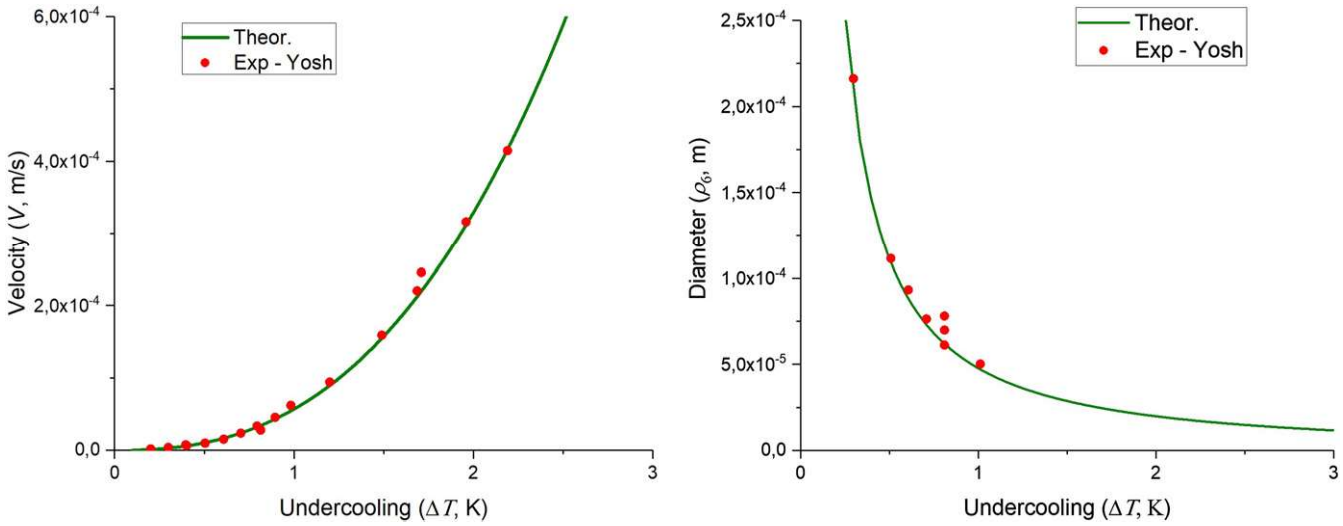

Figure 4. Theory versus experiments carried out by Yoshizaki *et al* [25] for the dendrite tip velocity V and its larger tip diameter ρ_6 as functions of the melt undercooling ΔT.

undercooling ΔT. The theory and experimental data are in good agreement in the range of small and moderate undercooling.

The smaller dendrite tip diameter ρ_2 was not directly measured but calculated following the results by Furukawa and Shimada [25, 32] as the direct ρ_2 data could not be obtained in the ISS (International Space Station) experiments. So, their semi-empirical law takes the form

$$\frac{\rho_2}{2d_0} = 425 \cdot \Delta^{-0.58}, \tag{9}$$

where $\Delta = \Delta T/T_{\mathrm{Q}}$ is the dimensionless undercooling. An important point is that this formula is a generalization of experimental data. The smaller tip diameter ρ_2 calculated on the

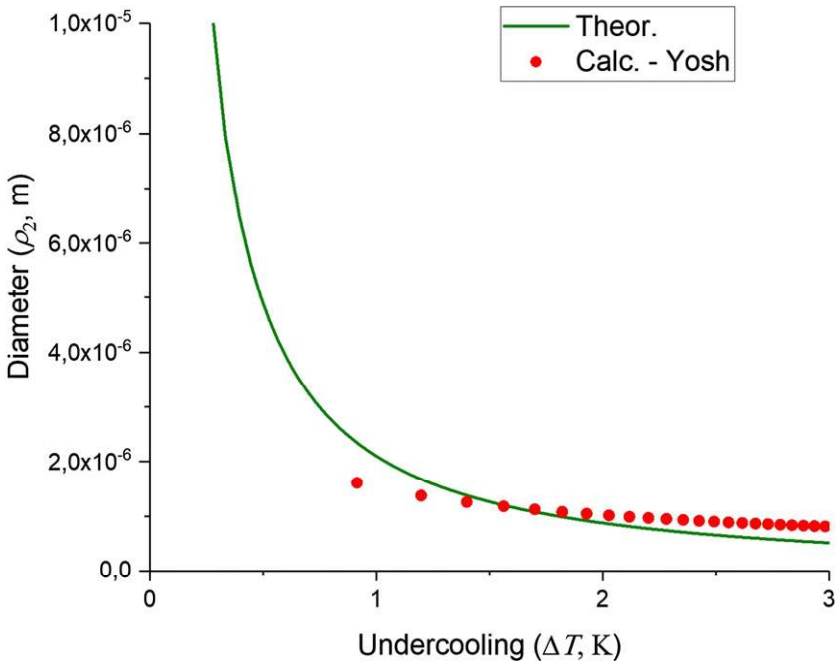

Figure 5. Theory versus data carried out by Yoshizaki *et al* [25] for the smaller dendrite tip diameter ρ_2 as a function of the melt undercooling ΔT.

basis of our theory (expressions (8)) as a function of the melt undercooling is compared with experimental data (expression (9)) in figure 5. A slight deviation of the curves is explained by the fact that the attitude of the dendrite could not be easily controlled in experiments [25].

4. Conclusion

In summary, the theory of stable three-dimensional dendritic growth in the form of an elliptical paraboloid is developed on the basis of undercooling balance condition and two stability criteria written out in two perpendicular dendritic planes (the basal plane described by the larger tip diameter ρ_6 and perpendicular to it plane described by the smaller tip diameter ρ_2). This theory leads to three non-linear algebraic equations determining three growth parameters—the dendrite tip velocity V and its tip diameters ρ_6 and ρ_2 as functions of the melt undercooling. The solution of these equations governing the stable growth mode is analytically found and tested against experimental data for ice crystals. We demonstrate that predictions of our theory agree well with experimental data in the range of small undercoolings. The theory is applicable for dendrites with non-axisymmetric morphology such as ice crystals with tip shapes of elliptical paraboloids.

Acknowledgments

The present research work consists of computational and theoretical parts, which were supported by different financial sources. In this connection, DVA acknowledges support from the Russian Foundation for Basic Research (Project No. 19-32-51009) for the derivation of model equations. LVT gratefully acknowledges research funding from the DAAD (Personal Ref. No.: 91687480) and the Ministry of Science and Higher Education of the Russian Federation (Project Passport No. 2338-21) within the 'Michael Lomonosov' programme scheme for solving the model equations and comparing them with experimental data. PKG and MR acknowledge support from German Space Center Space Management under Contract Number 50WM1541 and from the European Space Agency under Contract Number AO-2009-829 for the interpretation of the results.

Data availability statement

The data that support the findings of this study are available upon reasonable request from the authors.

Appendix. Boundary integrals for elliptical dendrites

Let us introduce how to derive the Horvay and Cahn solution describing the elliptical paraboloid from the boundary integral method. Horvay and Cahn [29] obtained the shape of an isothermal dendrite having an elliptical cross section. In this case the surface of the dendrite in dimensionless coordinates has the form (1). The dimensionless undercooling as a function of P_{T} can be written as [33]

$$\Delta - \frac{d_{\mathrm{c}}}{\rho}K - \beta V\left(1 + \frac{\partial\zeta(x,t)}{\partial t}\right) = I_{\zeta}^{T}, \qquad (10)$$

where (in dimensionless variables)

$$I_\zeta^T = \int_0^\infty \frac{\mathrm{d}\tau}{(2\pi\tau)^{3/2}} \int_{-\infty}^{\infty}\int_{-\infty}^{\infty} \mathrm{d}^2x_1 \left[1 + \frac{\partial\zeta(x_1, t-\tau)}{\partial t}\right] \times \exp\left\{-\frac{1}{2\tau}\left[|x-x_1|^2 + (\zeta(x,t) - \zeta(x_1, t-\tau) + \tau)^2\right]\right\}. \quad (11)$$

Here $\Delta = (T_\mathrm{m} - T_\infty)/T_\mathrm{Q}$ is the dimensionless undercooling, β is the kinetic coefficient, variables x, x_1 and ζ are measured in units of ρ/P_T, and variables t and τ are measured in units of $\rho/(P_\mathrm{T}V)$. Further, the substitution of interfacial function $\zeta = z$ from (1) leads to

$$I_\zeta^T = \left(\frac{1}{2\pi}\right)^{3/2} \int_0^\infty \frac{\mathrm{d}\tau}{\tau^{3/2}} \int_{-\infty}^{\infty}\int_{-\infty}^{\infty} \mathrm{d}x_1\,\mathrm{d}y_1 \times \exp\left\{-\frac{1}{2\tau}\left[(x-x_1)^2 + (y-y_1)^2 + \left(\frac{x_1^2 - x^2}{2(\omega-b)} + \frac{y_1^2 - y^2}{2(\omega+b)} + \tau\right)^2\right]\right\}. \quad (12)$$

Replacing two integration variables τ and y_1 by ω_1 and z_1 respectively as

$$\tau = \frac{(x-x_1)^2}{2\omega_1}, \quad y - y_1 = (x-x_1)z_1 \quad (13)$$

we can obtain

$$I_\zeta^T = \left(\frac{1}{\pi}\right)^{3/2} \frac{1}{2} \int_0^\infty \frac{\mathrm{d}\omega_1}{\sqrt{\omega_1}} \int_{-\infty}^{\infty} \exp(-\omega_1(1+z_1^2))\mathrm{d}z_1 \times \int_{-\infty}^{\infty} \exp\left\{-\omega_1\left(-\frac{x_1 + x}{2(\omega-b)} - \frac{z_1(2y - z_1(x-x_1))}{2(\omega+b)} + \frac{x-x_1}{2\omega_1}\right)^2\right\} \mathrm{d}x_1. \quad (14)$$

Integrating the right-hand side of equation (14) over x_1 and z_1 yields

$$I_\zeta^T = \sqrt{\omega+b} \int_0^\infty \frac{\exp\left((\omega+b)\left(1 + \frac{\omega_1}{\omega-b}\right) - \omega_1\right)}{\sqrt{\omega_1}\sqrt{1 + \frac{\omega_1}{\omega-b}}} \times \mathrm{erfc}\left(\sqrt{(\omega+b)\left(1 + \frac{\omega_1}{\omega-b}\right)}\right) \mathrm{d}\omega_1. \quad (15)$$

Where it has been taken into account the following [34]

$$\int_0^\infty \frac{\exp(-\mu^2u^2)\mathrm{d}u}{u^2 + \beta^2} = \frac{\pi}{2\beta}\mathrm{erfc}(\beta\mu)\exp(\beta^2\mu^2). \quad (16)$$

Replacing the variable ω_1 by $u = \sqrt{1 + \frac{\omega_1}{\omega-b}}$, we obtain

$$I_\zeta^T = 2\sqrt{\omega^2 - b^2}\,\exp(\omega - b)\,J(\omega), \quad (17)$$

where

$$J(\omega) = \int_1^\infty \frac{\exp\left(2bu^2\right)\mathrm{erfc}\left(u\sqrt{(\omega+b)}\right)\mathrm{d}u}{\sqrt{u^2-1}}. \quad (18)$$

Next, applying the method of differentiation and integration $J(\omega)$ and considering that

$$\int_1^\infty \frac{\exp(-\mu u)\mathrm{d}u}{\sqrt{u-1}} = \sqrt{\frac{\pi}{\mu}}\exp(-\mu), \quad (19)$$

we arrive at

$$I_\zeta^T = \sqrt{\omega^2 - b^2}\,\exp(\omega)\int_\omega^\infty \frac{\exp(-t)\,\mathrm{d}t}{\sqrt{t^2 - b^2}}. \quad (20)$$

Keeping in mind that at the interface $\omega = P_\mathrm{T}$ we obtain

$$\Delta T_\mathrm{T} = I_\zeta^T T_\mathrm{Q} = T_\mathrm{Q}\sqrt{P_\mathrm{T}^2 - b^2}\,\exp(P_\mathrm{T})\int_{P_\mathrm{T}}^\infty \frac{\exp(-y)\mathrm{d}y}{\sqrt{y^2 - b^2}}. \quad (21)$$

For $b = 0$, the cross-section is circular and one can obtain the Ivantsov's solution [13, 35].

ORCID iDs

L V Toropova https://orcid.org/0000-0003-4587-2630
D V Alexandrov https://orcid.org/0000-0002-6628-745X
P K Galenko https://orcid.org/0000-0003-2941-7742
G Demange https://orcid.org/0000-0002-1062-5181

References

[1] Kurz W and Fisher D J 1989 *Fundamentals of Solidification* (Aedermannsdorf: Trans. Tech. Publication)
[2] Trivedi R and Kurz W 1994 *Int. Mater. Rev.* **39** 49
[3] Galenko P K and Alexandrov D V 2018 *Phil. Trans. R. Soc.* A **376** 20170210
[4] Alexandrov D V and Zubarev A Y 2020 *Phil. Trans. R. Soc.* A **378** 20200002
[5] Alexandrov D V and Galenko P K 2020 *Phil. Trans. R. Soc.* A **378** 20190243
[6] Kessler D A, Koplik J and Levine H 1988 *Adv. Phys.* **37** 255
[7] Pelcé P and Bensimon D 1987 *Nucl. Phys.* B **2** 259
[8] Barbieri A and Langer J S 1989 *Phys. Rev.* A **39** 5314
[9] Brener E A and Mel'nikov V I 1991 *Adv. Phys.* **40** 53
[10] Ben Amar M and Pelcé P 1989 *Phys. Rev.* A **39** 4263
[11] Alexandrov D V, Galenko P K and Toropova L V 2018 *Phil. Trans. R. Soc.* A **376** 20170215
[12] Bouissou P and Pelcé P 1989 *Phys. Rev.* A **40** 6673
[13] Alexandrov D V and Galenko P K 2014 *Phys.-Usp.* **57** 771
[14] Alexandrov D V and Galenko P K 2015 *Phys. Chem. Chem. Phys.* **17** 19149
[15] Toropova L V, Alexandrov D V and Galenko P K 2020 *Math. Methods Appl. Sci.* **1**

[16] Toropova L V, Alexandrov D V, Rettenmayr M and Galenko P K 2020 *J. Cryst. Growth* **535** 125540
[17] Kao A, Toropova L V, Krastins I, Demange G, Alexandrov D V and Galenko P K 2020 *JOM* **72** 3123–31
[18] Galenko P K, Alexandrov D V and Titova E A 2018 *Phil. Trans. R. Soc.* A **376** 20170218
[19] Alexandrov D V and Galenko P K 2017 *Acta Mater.* **137** 64
[20] Alexandrov D V and Galenko P K 2019 *IUTAM Symp. Recent Advances in Moving Boundary Problems in Mechanics* vol 34 (Berlin: Springer) p 203
[21] Demange G, Zapolsky H, Patte R and Brunel M 2017 *Phys. Rev.* E **96** 022803
[22] Demange G, Zapolsky H, Patte R and Brunel M 2017 *Npj Comput. Mater.* **3** 1
[23] Kao A, Toropova L V, Alexandrov D V, Demange G and Galenko P K 2020 *J. Phys.: Condens. Matter.* **32** 194002
[24] Teraoka Y, Saito A and Okawa S 2002 *Int. J. Refrig.* **25** 218
[25] Yoshizaki I, Ishikawa T, Adachi S, Yokoyama E and Furukawa Y 2012 *Microgravity Sci. Technol.* **24** 245
[26] Alexandrov D V and Galenko P K 2017 *Europhys. Lett.* **119** 16001
[27] Toropova L V, Galenko P K, Alexandrov D V, Demange G, Kao A and Rettenmayr M 2020 *Eur. Phys. J. Spec. Top.* **229** 275
[28] Toropova L V, Galenko P K, Alexandrov D V, Rettenmayr M, Kao A and Demange G 2020 *Eur. Phys. J. Spec. Top.* **229** 2899
[29] Horvay G and Cahn J W 1961 *Acta Metall.* **9** 695
[30] Ben Amar M and Brener E 1993 *Phys. Rev. Lett.* **71** 589
[31] Titova E A, Alexandrov D V and Galenko P K 2020 *Eur. Phys. J. Spec. Top.* **229** 2891
[32] Furukawa Y and Shimada W 1993 *J. Cryst. Growth* **128** 234
[33] Alexandrov D V and Galenko P K 2017 *Physica* A **469** 420
[34] Gradshteyn I S and Ryzhik I M 2014 *Table of Integrals, Series, and Products* (New York: Academic)
[35] Ivantsov G P 1947 *Dokl. Akad. Nauk USSR* **58** 567